Improved tissue modelling and fast solver methods for high resolution FE-modelling in EEG/MEG-source localization

C.Wolters[1,2], S.Reitzinger[3], A.Basermann[4], S.Burkhardt[1,2],U.Hartmann[4], F.Kruggel[1] and A.Anwander[1]

[1]*Max-Planck-Institute of Cognitive Neuroscience, Leipzig, Germany,* [2]*Max-Planck-Institute for Mathematics in the Sciences, Leipzig, Germany,* [3]*SFB F013, "Numerical and Symbolic Scientific Computing", J.Kepler University, Linz, Austria,* [4]*C&C Research Laboratories, NEC Europe Ltd., St.Augustin, Germany,*

1 Introduction

The inverse problem in EEG and MEG amounts to finding a realistic source distribution in the human brain for a given set of field observations on the surface of the head. This requires the repeated solution of the forward problem, i.e., the simulation of the field propagation for a given dipolar source in the brain using a volume-conduction model of the head. For the most realistic modelling, the different tissues have to be segmented and assigned individual conductivity tensor material parameters. Layers like the skull or fibrous tissues like brain white matter are known to be anisotropic up to a ratio of 1:10. One of the most sensitive parameters is the anisotropic conductivity of the skull. The identification of the cerebrospinal fluid (CSF)-skull boundary based on T1-weighted MRI (T1-MRI) is problematic and Proton-Density-Weighting (PD-MRI) is most suitable for this task. In this paper we will outline how individualized high resolution finite element (FE) models, exploiting multimodal MR-imaging protocols, are automatically constructed. We present an improved segmentation of the skull through a combination of T1- and PD-MRI. The structural information about the white matter fibre directions are won through an MR-diffusion tensor imaging protocol [1]. The use of fast techniques to solve the large sparse systems of linear equations arising from the 3D FE method is necessary in order to have more acceptable solution times with high resolution anisotropic models and inverse source localization. Preconditioned Krylov-subspace-methods are among the most attractive iterative methods. We will compare incomplete threshold-factorization- with multigrid- preconditioners, the latter is known to be an optimal method with respect to the operation count and memory. Since the geometric construction of a grid-hierarchy is difficult (we only have tensor measurements for the finest level), we use a pure algebraic multigrid (AMG) preconditioner.

2 Methods

2.1 Segmentation and mesh generation

The following description summarizes the segmentation/registration-results obtained in [2]. A voxel-similarity based affine registration without pre-segmentation using a cost function based on mutual information was used to register the PD-MRI onto the corresponding T1-MRI. The maximization of the mutual information was carried out using a multilevel-downhill-simplex approach exploiting Freudenthal-triangulation, which turned out to be the most accurate and the fastest method compared to a genetic optimization approach or Powells direction set method. Initial skull surface segmentations were calculated using a fuzzy-C-means classification algorithm which corrects for intensity inhomogeneities in the MR-images. Within this procedure, the segmentation of the inner skull surface was obtained from the PD-image whereas for the outer skull surface both image modalities were exploited. The initial surfaces were triangulated and treated as a deformable model to obtain the final skull-segmentation result. The segmentation of CSF, white and grey matter was carried out following [3].

Motivated by the results of [4], a voxel-based mesh-generator [5] with and without surface-smoothing (node-shift) was developed to generate surface-smoothed hexahedra FE-meshes which better take into account the result of the accurate skull-segmentation.

2.2 Fast solver methods for FE-equations

A description of the multigrid-method as a preconditioner within a Krylov-subspace method can be found in [7]. [8] and [9] focus on incomplete factorization preconditioners and their parallelization.

The condition number of the symmetric positive-definite geometry-matrix A of the linear equation system $A\Phi = J$, with the given source J and the un-

Algorithm 1 Setup process for AMG: Setup(A_l,l)

if $|\omega_l| > COARSEGRID$ **then**
  Split ω_l into disjoint sets ω_C and ω_F
  Set $\omega_{l+1} = \omega_C$
  Define the interpolation operator P, $R = P^T$
  $A_{l+1} = RA_lP$
  Setup(A_{l+1},l+1)
else
  Perform an LL^t-factorization of A_l
  COARSELEVEL = l
end if

known potential Φ, is of order $\kappa(A) = \mathcal{O}(h^{-2})$, where h is the mesh-size of the FE mesh. A large condition number limits the accuracy and performance of Krylov-methods so that the goal of a preconditioner, M, is the reduction of $\kappa(M^{-1}A)$ for the preconditioned equation system $M^{-1}A\Phi = M^{-1}J$. A second requirement is that it is cheap to solve linear systems $Mz_j = r_j$ (z_j: residual for the preconditioned system, r_j: residual), needed in the j^{th} step of the iterative Krylov method. Up to now, we used "matrix-pattern" factorization preconditioners for the conjugate gradient (CG) method. The diagonal scaling or Jakobi-preconditioning chooses $M = D$ with D the diagonal entries of A. The IC(0)-factorization preconditioner exploits an incomplete Cholesky-decomposition $M = LL^t$ of A with zero fill-in, i.e., L has the same non-zero-pattern as A. Such factorizations are "blind" to numerical values because elements that are dropped depend only on the structure of A. In this paper, we tested a threshold-technique where elements are dropped according to their magnitude, the incomplete LDL^t fac. with threshold value ϵ (ILDLT(ϵ). The performance

Algorithm 2 V(ν_F,ν_B)-cycle: AMG(A_l, u_l, f_l,l)

if $l = COARSELEVEL$ **then**
  $u_l = (LL^t)^{-1} f_l$ (forward-back sweep)
else
  Relax ν_F times on $A_l u_l = f_l$
  Calculate the defect $d_l = f_l - A_l u_l$
  Restrict the defect $d_{l+1} = Rd_l$
  Set $u_{l+1} \equiv 0$
  Apply AMG(A_{l+1},u_{l+1},d_{l+1},l+1)
  Prolongate the correction $s_l = Pu_{l+1}$
  Update the solution $u_l = u_l + s_l$
  Relax ν_B times on $A_l u_l = f_l$
end if

Table 1: *Condition numbers of the different models.*

Model	eigenvalue largest	eigenvalue smallest	condition number
Rea-ns-cube	14.282	$0.506 * 10^{-6}$	$2.822 * 10^7$
Rea-cube	13.570	$0.494 * 10^{-6}$	$2.742 * 10^7$
4Sp-nscu-iso	8.114	$0.132 * 10^{-5}$	$6.147 * 10^6$
4Sp-nscu-ani	8.114	$0.126 * 10^{-5}$	$6.439 * 10^6$
4Sp-cu-iso	7.74	$0.13 * 10^{-5}$	$5.85 * 10^6$
4Sp-cu-ani	7.74	$0.12 * 10^{-5}$	$6.09 * 10^6$
4Sp-tet-iso	97.28	$0.62 * 10^{-5}$	$1.57 * 10^7$
4Sp-tet-ani	42.83	$0.56 * 10^{-5}$	$7.71 * 10^6$

of the ILDLT(ϵ)-CG method will be compared with an ILDLT(ϵ) preconditioned symmetric variant of the Quasi-Minimal Residual (QMR) algorithm derived in [9]. For factorization preconditioners, the system $Mz_j = r_j$ can be solved by a forward-back sweep.
The multigrid method requires $\mathcal{O}(N \log \eta^{-1})$ arithmetical operations to reduce the initial error by the factor η (N: problem size) [6]. The Multigrid-preconditioner leads to a condition number of $\mathcal{O}(1)$ [7]. The number of iterations is also independent of h. For the algebraic multigrid, these result have not yet been proved but they are accepted as 'empirical results'. In the following we are concerned with the construction of an AMG preconditioner. $A_h = A$ can be interpreted as an FE-grid, i.e., the diagonal entries of the matrix A_h are related to grid points in ω_h and off-diagonal entries are related to edges in an FE-mesh. First we investigate the coarsening process. Motivated from an FE mesh, the grid points ω_h (or equivalently the matrix A_h) can be split into two disjoint subsets $\omega_h = \omega_C \cup \omega_F$ such that there are (almost) no direct connections between any two coarse grid nodes and the resulting number of coarse grid nodes is as large as possible (for more detailed information see [10]). Next the prolongation operator P from a coarser to a finer grid has to be defined. The most simple prolongation and the one which turned out to be most efficient in our simulations is the 'equal distribution' which is given by

$$(P)_{ij} = \begin{cases} 1 & i = j \in \omega_C \\ \frac{1}{|\omega_C^i|} & i \in \omega_F, j \in \omega_C^i \\ 0 & otherwise \end{cases}$$

with $\omega_C^i = N^i \cap \omega_C$ and $N^i = \{j \,|\, |a_{ij}| > \delta \cdot |a_{ii}|\}$.

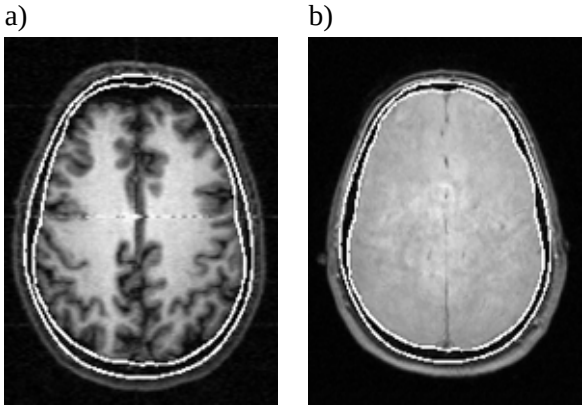

Figure 1: *Skull surface segmentation result through multimodal MR-imaging presented on underlying MR-images. a) T1-weighted b) registered PD-weighted*

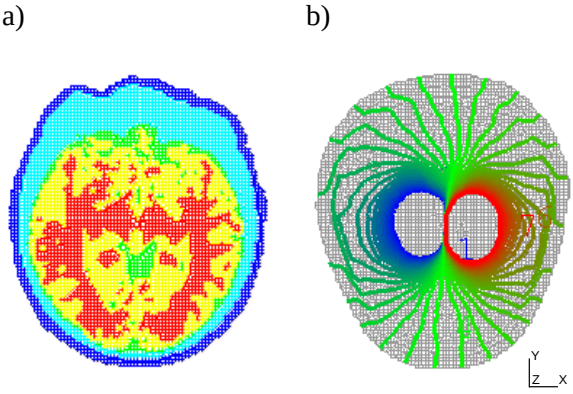

Figure 2: *a) Axial layer of the node-shifted FE-mesh of a realistic 5-tissue model. b) Isopotential-lines from $-2\mu V$ to $+2\mu V$ on a coronal layer of the node-shifted FE-mesh.*

The restriction operator is defined by $R := P^T$. With these definitions, the coarse grid operator A_H is realized by the classical Galerkin method $A_H = RA_hP$ and a recursive application of the above steps immediately leads to a multilevel setup (Alg. 1). Finally an appropriate smoother is defined by a Gauß-Seidel method and thereafter a usual multigrid cycle is given in Alg. 2. For the m-V(ν_F,ν_B) cycle AMG preconditioned CG method, the preconditioning operation $Mz_j = r_j$ is equivalent to m calls of AMG(A,z_j,r_j,1) where the current z_j is always used.

3 Results

3.1 Segmentation and mesh generation

The results obtained by the procedure described in Section 2.1 are shown in the Fig. 1 and 2a.

3.2 Solver-comparison

The isotropic conductivity values of the 5-tissue realistic head model were chosen as follows (in S/m): skin 0.33, skull 0.0042, CSF 1.0, grey matter 0.33 and white matter 0.14. Isotropic (Rea-cube) and node-shifted (Rea-ns-cube) 2mm cube meshes were generated. A 4-layer sphere model (cond. 0.33, 0.0042, 1.0 and 0.33) was constructed and meshed with 2mm isotropic (4Sp-cu-iso) and 2mm node-shifted (4Sp-nscu-iso) cube elements. A radial:tangential anisotropy of 1:10 was assigned for the "skull" layer (4Sp-nscu-ani, 4Sp-cu-ani). A geometry-based mesh generator was used to generate a tetrahedral mesh for the isotropic (4Sp-tet-iso) and anisotropic (4Sp-tet-ani) 4-layer-sphere model. After setting up the geometry matrices, the condition numbers, defined as the quotient of largest over smallest eigenvalue, were calculated to obtain an impression about the ill-posedness using the algorithms described in [9]. The solver-performance tests were carried out on a 1-processor-machine (CPU: MIPS R10000,180MHz, FPU: MIPS R10010, 2MB sec.cache, 32KB instruction and 32KB data cache). The starting vector for all solvers was $\mathbf{0}$. Since the solver-performance diagrams were quite comparable for all tested equation systems, only two representative figures are presented (Fig. 3 and 4). The selected values of δ in the AMG- and ϵ in the threshold-case are indicated behind the preconditioner, the number of iterations can be found behind the Krylov-method. We used the 1-V(1,1)-cycle-AMG-preconditioner. The setup-times for the preconditioners were neglected since it has to be performed only once for the inverse problem. To give an example, the AMG in Fig. 3 used 6 levels with sizes 323752, 57929, 8613, 2146, 1126 and 687. The setup-time was 80.2 seconds. The setup-time for the ILDLT(1e-3)-preconditioner was 37.8 seconds.

4 Discussion

The subject in Fig. 1 shows an above-average amount of CSF. A segmentation of the inner skull surface based on only the T1-weighted MRI would be especially flawed in such cases and could lead to large mislocalizations [11].

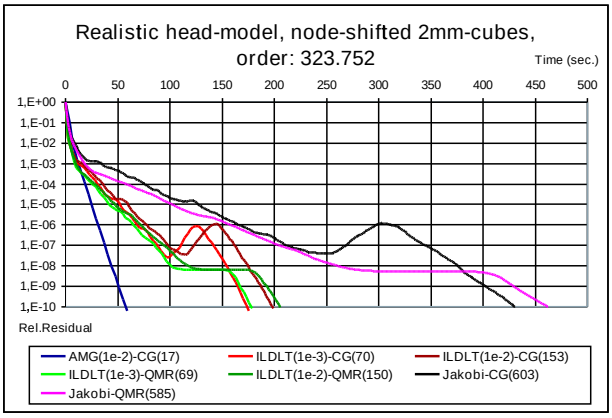

Figure 3: *Solver comparison (L_2-relative residual).*

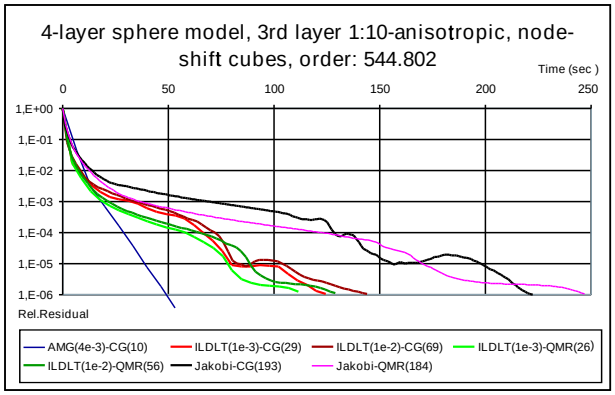

Figure 4: *Solver comparison (L_2-relative residual).*

The results in Table 1 show a minor influence of the modelled anisotropy and the node-shift on the condition number. The performance tests with ILDLT- and AMG-preconditioning, both taking anisotropy into account, showed no remarkable difference in the solver times. The calculation times of the Jakobi-preconditioned Krylov-solvers were up to a factor 1.25 longer for the anisotropic models, probably because of less-clustered eigenvalue spectra. Up to a relative L_2-residual of 10^{-3}, the differences between the ILDLT- and the AMG-preconditioned Krylov methods are minimal. From 10^{-5} up to 10^{-10}, the AMG-preconditioned CG method is the fastest in all tested cases and a factor 2 to 3 times faster than the best-tuned ILDLT-preconditioned Krylov method. Because of the loss of about 3 digits for the potential from the source to the electrodes, the interesting residuals begin at about 10^{-5}. For very small residuals, the ILDLT-CG shows peaks where the ILDLT-QMR has a plateau. This is surely due to the different minimization criteria of both Krylov-methods (the CG-method tries to minimize the A-energy-norm whereas the QMR method minimizes the L_2-norm which has been visualized in the figures). In future examinations, we will include skull-anisotropy and the white-matter tensor measurements, described in [1]. Because these tensors change from element to element, it can be assumed that the eigenvalue spectra are more strongly 'blurred' than in the tested models. We conclude that with regard to the inverse problem, acceptable calculation times can only be reached through a parallelization of the presented solvers.

Acknowledgements

This work was supported by the Leibniz-Prize of the German Research Foundation awarded to Prof.A.D.Friederici, by Prof.E.Zeidler, by the IST-program of the European Community, project SIM-BIO, and by the Austrian Science Foundation (FWF).

References

[1] C.Wolters et al., in *4th Symp. on Comp. Meth. in Biomech. and Biomed.Eng., Lisboa,Portugal, 1999*, J.Middleton, Ed., to appear.

[2] S.Burkhardt, Diplomarbeit, Fak. für Mathematik und Informatik, Uni. Leipzig, 2000.

[3] F.Kruggel and D.Y. von Cramon, *Medical Image Analysis* **3**(2), 1–11, 1999.

[4] D.Camacho et al., *J.Biomechanics* **30**(10), 1067–1070, 1997.

[5] U.Hartmann and F.Kruggel, *Comp. Meth. in Biomech. and Biomed. Eng.* **2**(1), 49–64, 1998.

[6] W. Hackbusch, Springer Verlag, 1985.

[7] M.Jung and U.Langer, *Surv.Math.Ind.* **1**, 217–257, 1991.

[8] Y.Saad, *PWS Publishing Company*, 1996.

[9] Basermann, A., *Num.Lin.Alg.with Appl.*, to appear.

[10] J. W. Ruge and K. Stüben, in *Multigrid Methods, Frontiers in Applied Mathematics*, S. McCormick, Ed., Philadelphia: SIAM, 1986, 73–130.

[11] G. Huiskamp et al., *IEEE Trans. Biomed.Eng.* **46**(11), 1281–1287, 1999.